Semimicroscopical description of the simplest photonuclear reactions accompanied by excitation of the giant dipole resonance in medium-heavy mass nuclei

V. A. Rodin[1,2] and M. H. Urin[2]
[1]*Institut für Theoretische Physik der Universität Tübingen, Auf der Morgenstelle 14, D-72076 Tübingen, Germany*
[2]*Department of Theoretical Nuclear Physics, Moscow Engineering and Physics Institute (State University), 115409 Moscow, Russia*
(Received 8 April 2002; published 30 December 2002)

A semimicroscopical approach is applied to describe photoabsorption and partial photonucleon reactions accompanied by the excitation of the giant dipole resonance (GDR). The approach is based on the continuum random phase approximation (CRPA) with a phenomenological description for the spreading effect. The phenomenological isoscalar part of the nuclear mean field, momentum-independent Landau-Migdal particle-hole interaction, and separable momentum-dependent forces are used as input quantities for the CRPA calculations. The experimental photoabsorption and partial (n,γ)-reaction cross sections in the vicinity of the GDR are satisfactorily described for ^{89}Y, ^{140}Ce, and ^{208}Pb target nuclei. The total direct-neutron-decay branching ratio for the GDR in ^{48}Ca and ^{208}Pb is also evaluated.

DOI: 10.1103/PhysRevC.66.064608 PACS number(s): 25.20.−x, 21.60.Cs, 21.60.Jz, 24.30.Cz

I. INTRODUCTION

A detailed description of the familiar (isovector, $T_3=0$) giant dipole resonance (GDR) in medium-heavy mass nuclei is a long-standing theoretical problem. A number of macroscopical, semiclassical, and microscopical approaches have been used to describe the photoabsorption cross section, the latter being proportional to the energy-weighted isovector dipole strength function [1]. Continuum random phase approximation (CRPA) -based microscopical approaches have been developed during the last two decades to describe the E1 strength function [2–5]. However, partial photonucleon reactions accompanied by the GDR excitation have not been studied in these approaches. Experimental data on these reactions (mainly on the neutron radiative capture) are usually described within the direct + semidirect capture model. The model was originally proposed by Brown [6] and substantially extended by the Lublyana group (see, e.g., Ref. [7], and references therein). Within the model a number of phenomenological quantities are used to parametrize the energy-averaged reaction amplitude and, in particular, a rather large imaginary part of the GDR form factor is used without a clear physical understanding of the origin of this part.

Partial photonuclear reactions accompanied by GDR excitation are closely related to GDR direct decay into the respective nucleon channels and carry information on the GDR structure. Therefore, the CRPA-based microscopical approaches, which are able to describe direct-nucleon decays of the GDR (see, e.g., Ref. [5]), can be extended to describe the partial photonucleon reactions.

An attempt to use the CRPA-based semimicroscopical approach to describe partial photonucleon reactions accompanied by the GDR excitation was undertaken in Ref. [8]. Later the approach was extended and applied by Urin and coworkers for describing the direct-nucleon-decay properties of a number of charge-exchange (isovector) and isoscalar giant resonances (see Refs. [9] and [10], respectively). The ingredients of the semimicroscopical approach are the following:

(i) the phenomenological isoscalar part of the nuclear mean field (including the spin-orbit term) and the momentum-independent Landau-Migdal particle-hole interaction, together with some partial self-consistency conditions;

(ii) a phenomenological account of the spreading effect (that is due to coupling of particle-hole-type doorway states to many-quasiparticle configurations) in terms of an energy-dependent smearing parameter.

However, it was found in Ref. [8] that the GDR energy and also the photoabsorption cross section integrated over the GDR region, σ^{int}_{GDR}, are noticeably underestimated in the calculations as compared with the respective experimental values [11]. The experimental value of σ^{int}_{GDR}, which exceeds the Thomas-Reiche-Kuhn (TRK) sum rule, $\sigma^{int}_{TRK}=60\ (NZ/A)$ MeV mb, can be reproduced in selfconsistent calculations provided momentum-dependent forces are taken into account. In Ref. [12] we provided a satisfactory description of the experimental GDR energy in ^{208}Pb and some partial ^{208}Pb(n,γ)-reaction cross sections in the GDR region by incorporating separable isovector momentum-dependent forces with the intensity normalized to describe the experimental σ^{int}_{GDR} value and without the use of additional adjustable parameters.

In the present work we extend the approach of Ref. [12] as follows. First, we use a simpler phenomenological realization for the spreading effect by introducing an energy-dependent smearing parameter directly into the CRPA equations. Secondly, we take into consideration also the isoscalar part of momentum-dependent forces in terms of an effective nucleon mass. Thirdly, the photonucleon-reaction cross sections are calculated for a number of nuclei and the results are compared with available experimental data. We also make predictions for several partial (γ,n)-reaction cross sections in the vicinity of the GDR in ^{208}Pb and, consequently, calculate partial direct-neutron decay branching ratios for this giant reasonance (GR). The total branching ratio is also evaluated for the GDR in ^{48}Ca and compared with recent $(e,e'n)$-reaction data [13].

II. BASIC EQUATIONS

The CRPA equations are given below in the form adopted from the Migdal's finite- Fermi-system theory [14]. Similar to Refs. [8,12], the isobaric structure of the GDR can be simplified by using the quantity $D_z=\Sigma_a d_z(a)$, with $d_z=-\frac{1}{2}\tau^{(3)}z$ as the z-projection of the dipole operator in the limit $(N-Z)/A\ll 1$. The photoabsorption cross section, $\sigma_a(\omega)$ (ω is the gamma-quantum energy), is then proportional to the dipole strength function $S(\omega)$:

$$\sigma_a(\omega)=B\omega S(\omega) \tag{1}$$

with $B=4\pi^2(e^2/\hbar c)$. Within the CRPA the strength function is determined by the effective dipole operator $\tilde{d}_z(\omega)$, which differs from d_z due to polarization effects caused by the particle-hole interaction $\hat{F}=\frac{1}{2}\Sigma_{1\neq 2}F(1,2)$. Together with the momentum-independent isovector part of the Landau-Migdal interaction, $F_{L-M}(1,2)=F'\cdot(\vec{\tau}_1\vec{\tau}_2)\delta(\vec{r}_1-\vec{r}_2)$, we also use translationally invariant separable momentum-dependent forces:

$$\hat{F}_{m-d}=-\frac{1}{4mA}\sum_{1,2}[\kappa_0+\kappa'(\vec{\tau}_1\vec{\tau}_2)](\vec{p}_1-\vec{p}_2)^2 \simeq -\frac{\kappa_0}{2m}\sum_1 \vec{p}_1^{\,2}+\frac{\kappa'}{2mA}\sum_{1,2}(\vec{\tau}_1\vec{\tau}_2)(\vec{p}_1\vec{p}_2), \tag{2}$$

where m is the nucleon mass, A is the number of nucleons, and κ_0 and κ' are the isoscalar and isovector strengths of the momentum-dependent forces, respectively. The approximate equality in Eq. (2) is valid provided that the isovector 1^- excitations are analyzed within the limit $(N-Z)/A\ll 1$.

The use of momentum-dependent forces approximated by Eq. (2) allows one to

(i) obtain simple expressions for the effective mass, $m^*=m/(1-\kappa_0)$, and also for the sum rule $\sigma^{int}=\int\sigma_a(\omega)d\omega=(1-\kappa_0)(1+\kappa')\sigma^{int}_{TRK}$;

(ii) use the following expression for $\tilde{d}_z(\omega)$:

$$\tilde{d}_z(\omega)=-\frac{1}{2}\tau^{(3)}\left[V(r;\omega)\frac{z}{r}+\frac{i}{\hbar}\Delta(\omega)p_z\right]. \tag{3}$$

Having separated isobaric and spin-angular variables in the CRPA equations, the following expressions for $S(\omega)$ and the components of the effective dipole operator within the above-mentioned approximation can be obtained:

$$S(\omega)=-\frac{2}{3}\mathrm{Im}\int r[A(r,r';\omega)+A_\kappa(r,r';\omega)]V(r';\omega)drdr', \tag{4}$$

$$A_\kappa(r,r';\omega)=-\frac{\kappa\int A(r,r';\omega)\hat{L}(r')dr'\int\hat{L}(r)A(r,r';\omega)dr}{1+\kappa\int\hat{L}(r)A(r,r';\omega)\hat{L}(r')drdr'}, \tag{5}$$

$$V(r;\omega)=r+\frac{2F'}{r^2}\int[A(r,r';\omega)+A_\kappa(r,r';\omega)]V(r';\omega)dr', \tag{6}$$

$$\Delta(\omega)=-\frac{\kappa\int\hat{L}(r)A(r,r';\omega)V(r';\omega)drdr'}{1+\kappa\int\hat{L}(r)A(r,r';\omega)\hat{L}(r')drdr'}, \tag{7}$$

where $\kappa=8\pi\hbar^2\kappa'/3mA$, and the operator $\hat{L}(r)$ is defined in terms of spin-angular matrix elements as follows: $\langle(\lambda)\|\hat{L}(r)\|(\lambda')\rangle=(\partial/\partial r)+[B_{(\lambda)(\lambda')}/r]$ with $(\lambda)=\{j_\lambda,l_\lambda\}$, $B_{(\lambda')(\lambda)}=[l_\lambda(l_\lambda+1)-l_{\lambda'}(l_{\lambda'}+1)]/2$. Furthermore, $A(r,r';\omega)=\frac{1}{2}(A^n+A^p)$, where $(rr')^{-2}A^\alpha(r,r';\omega)$ is the radial part of the free particle-hole propagator carrying the GDR quantum numbers ($\alpha=n,p$). The propagators A^α can be presented in the following form:

$$A^\alpha(r,r';\omega)=\sum_{\mu,(\lambda)}[t^{(1)}_{(\lambda)(\mu)}]^2 n^\alpha_\mu \times[\chi^\alpha_\mu(r)g^\alpha_{(\lambda)}(r,r';\varepsilon_\mu+\omega)\chi^\alpha_\mu(r') +\chi^\alpha_\mu(r')g^\alpha_{(\lambda)}(r',r;\varepsilon_\mu-\omega)\chi^\alpha_\mu(r)], \tag{8}$$

where $\mu=\{\varepsilon_\mu,(\mu)\}$ is the set of quantum numbers for single-particle bound states; $t^{(L)}_{(\lambda)(\mu)}=\langle(\lambda)\|Y_L\|(\mu)\rangle/\sqrt{2L+1}$ is the kinematic factor {the definition of the reduced matrix elements $\langle(\lambda)\|Y_L\|(\mu)\rangle$ is taken in accordance with Ref. [15]}, $n_\mu=N_\mu/(2j_\mu+1)$ is the occupation factor (N_μ is the number of nucleons occupying level μ), $r^{-1}\chi^\alpha_\mu(r)$ is the bound-state radial wave function, and $(rr')^{-1}g^\alpha_{(\lambda)}(r,r',\omega)$ is the Green's function of the single-particle radial Schrödinger equation.

A realization of the optical theorem follows from Eqs. (1)–(8):

$$\sigma_a(\omega)=\sum_{\mu(\lambda)\alpha}\sigma_{\mu(\lambda)\alpha}(\omega);\quad \sigma_{\mu(\lambda)\alpha}(\omega)=|M_{\mu(\lambda)\alpha}(\omega)|^2; \tag{9}$$

$$M_{\mu(\lambda)\alpha}(\omega)=\left(\frac{\pi}{3}B\omega n^\alpha_\mu\right)^{1/2}t^{(1)}_{(\lambda)(\mu)}\int\chi^{(+)\alpha}_{\varepsilon(\lambda)}(r)[V(r,\omega)+\Delta(\omega)\hat{L}(r)]\chi^\alpha_\mu(r)dr. \tag{10}$$

In Eq. (9), σ_c is the double partial (γ,N)-reaction cross section, and $c=\{\mu(\lambda)\alpha\}$ is a set of channel quantum numbers. Therefore, $\sigma_{\mu\alpha}(\omega)=\Sigma_{(\lambda)}\sigma_{\mu(\lambda)\alpha}(\omega)$ is the partial cross section corresponding to the population of the one-hole state μ in the α subsystem of the product nucleus (only nuclei without nucleon pairing are considered). In Eq. (10), $r^{-1}\chi^{(+)\alpha}_{\varepsilon(\lambda)}$ is the radial scattering wave function (normalized to the δ function of energy) with the escape-nucleon energy given by $\varepsilon=\varepsilon^{\alpha}_{\mu}+\omega$.

The formula for the cross section of the inverse reaction (nucleon radiative capture by closed-shell nuclei) is derived using the detailed balance principle:

$$\sigma^{inv}_{c}(\omega)=(\omega^2/2mc^2\varepsilon)\sigma_c(\omega);\quad \sigma^{inv}_{\mu\alpha}=\sum_{(\lambda)}\ \sigma^{inv}_{\mu(\lambda)\alpha}, \tag{11}$$

where ε is the kinetic energy of the captured nucleon. In deriving these formulas (in which both σ_c's correspond to the same compound nucleus) we neglect the difference between the effective dipole operators calculated for the A and $A+1$ nuclei: this assumption is expected to be valid with an accuracy of $A^{-2/3}$. Also, we note that the quantities $\sigma_{\mu(\lambda)\alpha}$ should be calculated by setting $n_\mu=1$ in Eq. (10), as follows from the consideration of kinematics of the (n,γ) reaction on closed-shell target nuclei.

The amplitudes $M_{\mu(\lambda)\alpha}$ in Eq. (10) also determine the anisotropy parameters, $a_{\mu\alpha}$, in the gamma-quantum angular distribution: $4\pi(d\sigma^{inv}_{\mu\alpha}/d\Omega)(\varepsilon,\theta)=\sigma^{inv}_{\mu\alpha}(\varepsilon)[1+a_{\mu\alpha}P_2(\theta)]$, where P_2 is the second degree Legendre polynomial. The expression for $a_{\mu\alpha}$ can be presented in the form:

$$a_{\mu\alpha}=-\sqrt{30\pi}\sum_{(\lambda)(\lambda')} i^{l_\lambda-l_{\lambda'}}W(2j'_\lambda 1 j_\mu; j_\lambda 1)\times t^{(2)}_{(\lambda)(\lambda')}(M_{c'})^{*}M_c \Big/ \sum_{(\lambda)}|M_c|^2, \tag{12}$$

where $W(abcd,ef)$ is a Racah coefficient and $c'=\alpha,\mu,(\lambda')$.

We emphasize that the above-mentioned expressions for the reaction amplitudes and cross sections are obtained within the CRPA. To calculate the energy-averaged amplitudes accounting for the spreading effect, we solve Eqs. (4)–(8) and (10) with the replacement of ω by $\omega+(i/2)I(\omega)$. The form of the smearing parameter $I(\omega)$ (the mean doorway-state spreading width) is taken to be similar to that obtained for the imaginary part of the nucleon-nucleus potential in some versions of the optical model (see, e.g., Ref. [16]), namely

$$I(\omega)=\alpha(\omega-\Delta)^2/[1+(\omega-\Delta)^2/B^2], \tag{13}$$

where α, Δ, and B are adjustable parameters. A reasonable description of the GR total width was obtained in Refs. [9,10], and also in Ref. [12] by using the parametrization given by Eq. (13). The approach described above allows one to calculate the energy-averaged photoabsorption cross section $\overline{\sigma}_a(\omega)$ and reaction amplitudes $\overline{M}_c$. The partial photonucleon-reaction cross sections $\overline{\sigma}_{\mu\alpha}$, $\overline{\sigma}^{inv}_{\mu\alpha}$ and anistropy parameters $\overline{a}_{\mu\alpha}$ are determined by the averaged amplitudes in the same way, as given by Eqs. (10)–(12), provided that the fluctuational part of the cross sections is neglected. Cross sections $\overline{\sigma}_{\mu\alpha}(\omega)$ determine the partial direct-nucleon-decay branching ratios, $b_{\mu\alpha}$, for the GDR according to the relation:

$$b_{\mu\alpha}=\int\overline{\sigma}_{\mu\alpha}(\omega)d\omega\Big/\int\overline{\sigma}_a(\omega)d\omega, \tag{14}$$

where integration is performed over the GDR region.

TABLE I. Model parameters U_0 and κ' used in calculations.

Nucleus	m^*/m	U_0 (MeV)	κ'
^{89}Y	1.0	53.3	0.53
	0.9	58.0	0.38
^{140}Ce	1.0	53.7	0.56
	0.9	57.9	0.39
^{208}Pb	1.0	53.9	0.56
	0.9	58.9	0.42
^{48}Ca	1.0	54.3	0.48

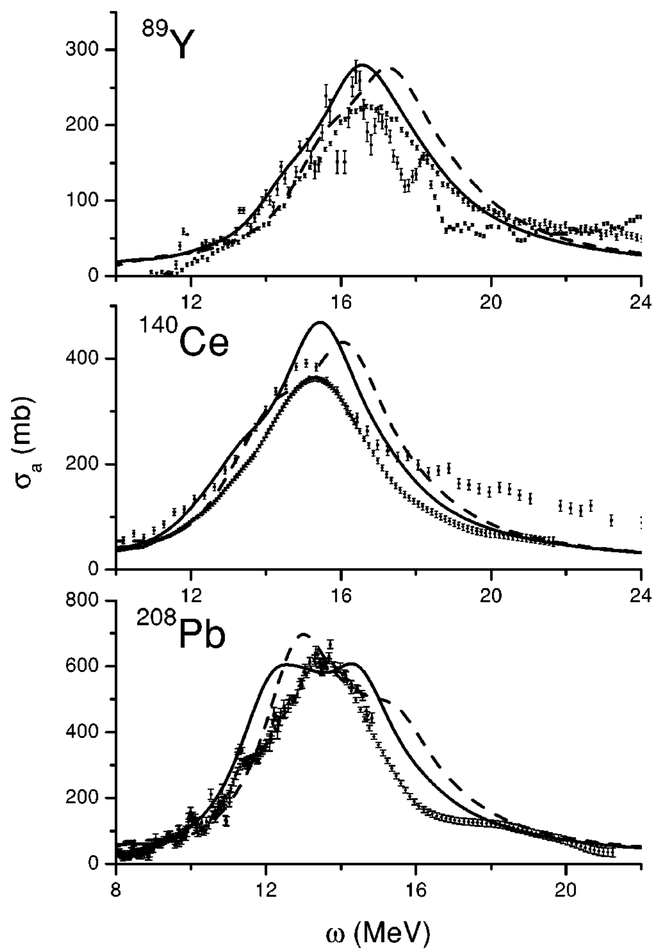

FIG. 1. The calculated photoabsorption cross sections, $\overline{\sigma}_a$, for ^{89}Y, ^{140}Ce, and ^{208}Pb (hereafter the solid and dashed lines correspond to calculations with $m^*/m=1$ and 0.9, respectively). The experimental data (black squares and circles) are taken from Ref. [11].

TABLE II. Spectroscopic factors of the valence-neutron states in ^{90}Y, ^{141}Ce, and ^{209}Pb (taken from the Ref. [7]).

^{90}Y		^{141}Ce		^{209}Pb	
μ	S_μ	μ	S_μ	μ	S_μ
$1g_{7/2}$	0.6	$2f_{5/2}$	0.8	$3d_{3/2}$	0.9
$2d_{3/2}$	0.7	$1h_{9/2}$	1.0	$2g_{7/2}$	0.8
$1h_{11/2}$	0.4	$1i_{13/2}$	0.6	$4s_{1/2}$	0.9
$3s_{1/2}$	1.0	$3p_{1/2}$	0.4	$3d_{5/2}$	0.9
$3d_{5/2}$	1.0	$3p_{3/2}$	0.4	$1j_{15/2}$	0.5
		$2f_{5/2}$	0.8	$1i_{11/2}$	1.0
				$2g_{9/2}$	0.8

III. CALCULATIONAL INGREDIENTS AND RESULTS

The experimental data on partial photonucleon reactions accompanied by the GDR excitation in medium-heavy mass nuclei are very scarce. Only available are two sets of the experimental data on the neutron radiative capture with GDR excitation in ^{208}Pb [17]. and in ^{89}Y and ^{140}Ce [18]. Before going to the results of the semimicroscopical description of these and some other data, we would like to comment on the ingredients of the approach and the smearing procedure.

As in Refs. [9,10], the nuclear mean field is taken as the sum of the isoscalar (including the spin-orbit term), isovector, and Coulomb terms:

$$U(x)=U_0(r)+U_{so}(r)\vec{\sigma}\vec{l}+\frac{1}{2}\tau^{(3)}v(r)+\frac{1}{2}[1-\tau^{(3)}]U_c(r), \tag{15}$$

with $U_0(r)=-U_0 f_{WS}(r,R,a)$ and $U_{so}(r)=-U_{so}df_{WS}(r)/rdr$, where f_{WS} is the Woods-Saxon function with $R=r_0A^{1/3}$, $r_0=1.24$ fm, $a=0.63$ fm, and $U_{so}=13.9[1+2(N-Z)/A]$ MeV fm^2. The symmetry potential $v(r)$ in Eq. (15) is calculated in a self-consistent way: $v(r)=2F'\rho^{(-)}$, where $\rho^{(-)}=\rho^n-\rho^p$ is the neutron excess density, and $F'=300f'$ MeV fm^3 with the Landau-Migdal parameter $f'=1.0$. The Coulomb part in Eq. (15) is calculated in the Hartree approximation via the proton density ρ^p. The isoscalar mean-field depth U_0 is chosen to describe experimental nucleon separation energies in the nuclei under consideration and depends on the choice of the effective mass [or parameter κ_0 in Eq. (2)]. In our calculations we used $m^*=m$ and also the "realistic" value $m^*=0.9\ m$. The extracted values of U_0 are

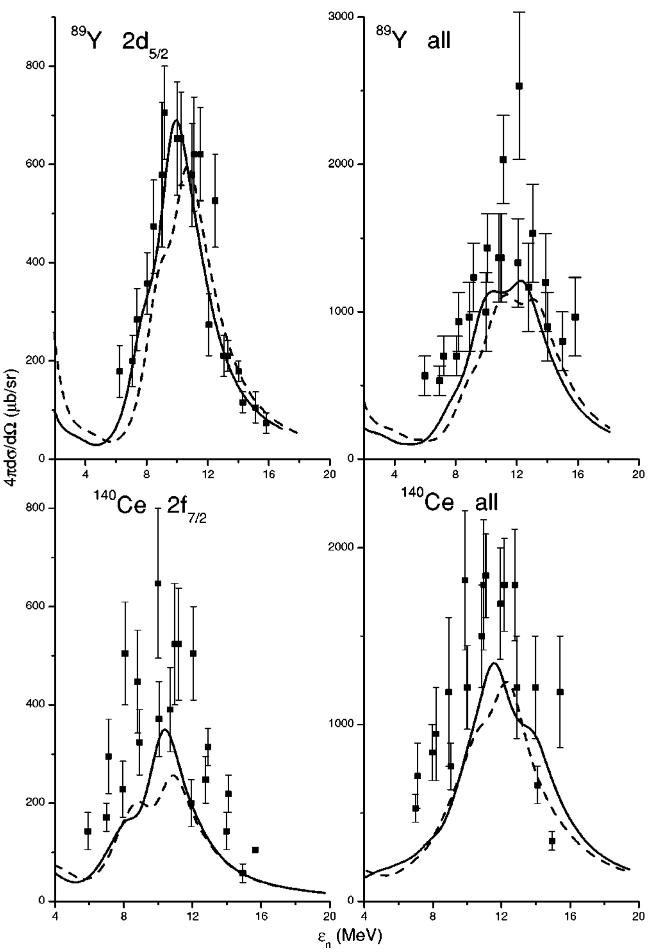

FIG. 2. The calculated partial cross sections at 90° multiplied by 4π as functions of neutron energy for neutron radiative capture to the ground state and to all the single-particle states in ^{90}Y and ^{141}Ce. The experimental data are taken from Ref. [18].

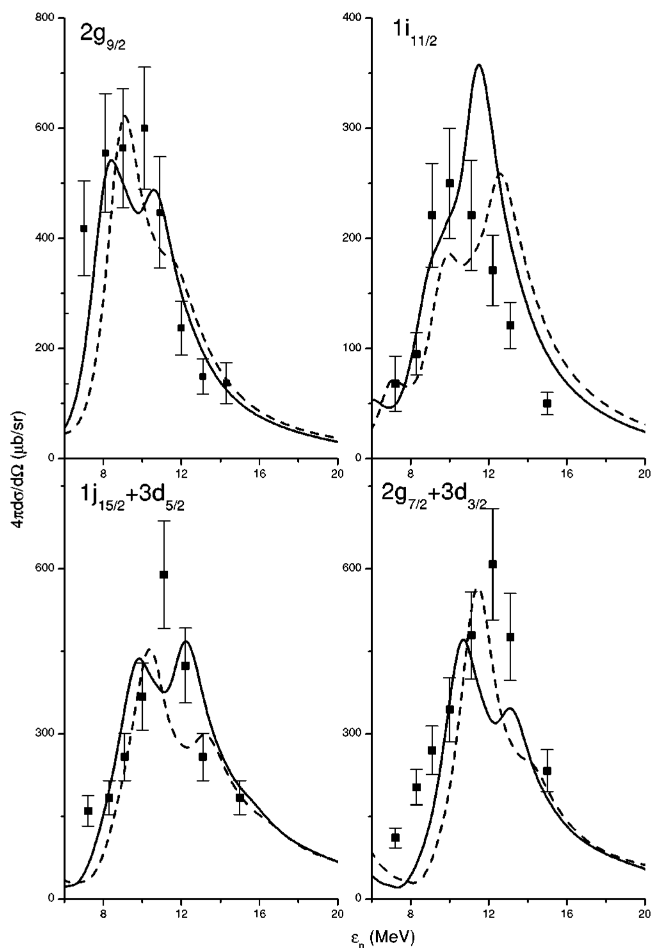

FIG. 3. The calculated partial cross sections at 90° multiplied by 4π as functions of neutron energy for neutron radiative capture to some single-particle states in ^{209}Pb. The experimental data are taken from Ref. [17].

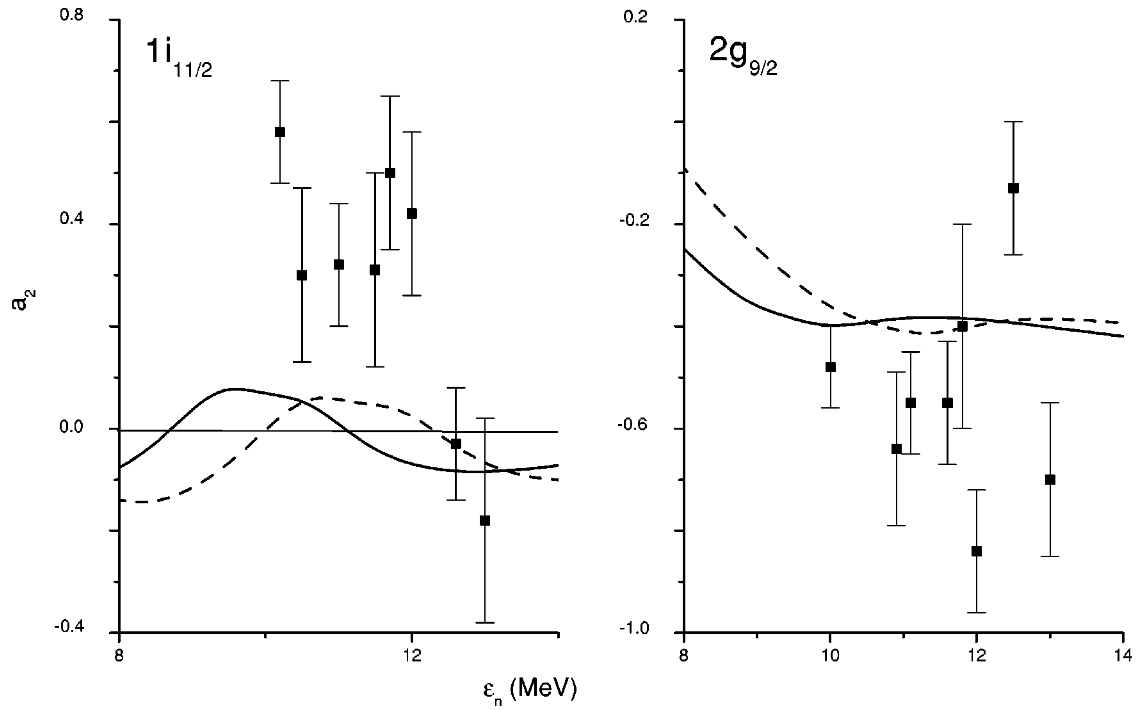

FIG. 4. Calculated anisotropy parameter a_2 for some partial ^{208}Pb(n,γ) reactions. The experimental data are taken from Ref. [17].

listed in Table I. The proton pairing in ^{89}Y and ^{140}Ce is approximately taken into account within the BCS model to calculate only the proton separation energy. In these calculations the pairing gap is determined from the experimental pairing energies.

To apply the smearing procedure, we calculate the ω-dependent single-particle quantities in Eqs. (8) and (10) (Green's functions and continuum-state wave functions) using the single-particle potential $U(x) \mp (i/2)I(\omega)f_{WS}(r,R^*,a)$. The cutoff radius is chosen as $R^*=2R$ in calculations of the Green's functions (i.e., in calculations of the effective dipole operator and, therefore, the strength function) and $R^*=R$ in calculations of the partial reaction-amplitudes. Such a choice of R^* makes the model more consistent in the region of the respective single-particle resonance. The parameters $\Delta=3$ MeV and $B=7$ MeV in Eq. (13) are taken to be the same as in Refs. [9,10,12], while parameters $\alpha=0.06$ MeV and κ' from Eq. (2), are chosen to describe the experimental total width and the energy of the GDR, respectively, in the nuclei under consideration. The κ' values are listed in Table I: as can be seen from the table, the model parameters used in our calculations are rather stable.

The quality of description of the experimental photoabsorption cross sections can be seen in Fig. 1, where the calculated cross sections $\overline{\sigma}_a(\omega)$ are shown for ^{89}Y, ^{140}Ce, and ^{208}Pb target nuclei. It is worth mentioning that the use of two adjustable parameters κ' and α allows one to satisfactorily describe three GDR parameters, namely, the energy, the total width, and the value of σ_{GDR}^{int}.

The energy-averaged differential partial cross sections for neutron radiative capture, $d\overline{\sigma}_{\mu}^{inv}/d\Omega$, are calculated without the use of any new adjustable parameters. Each calculated

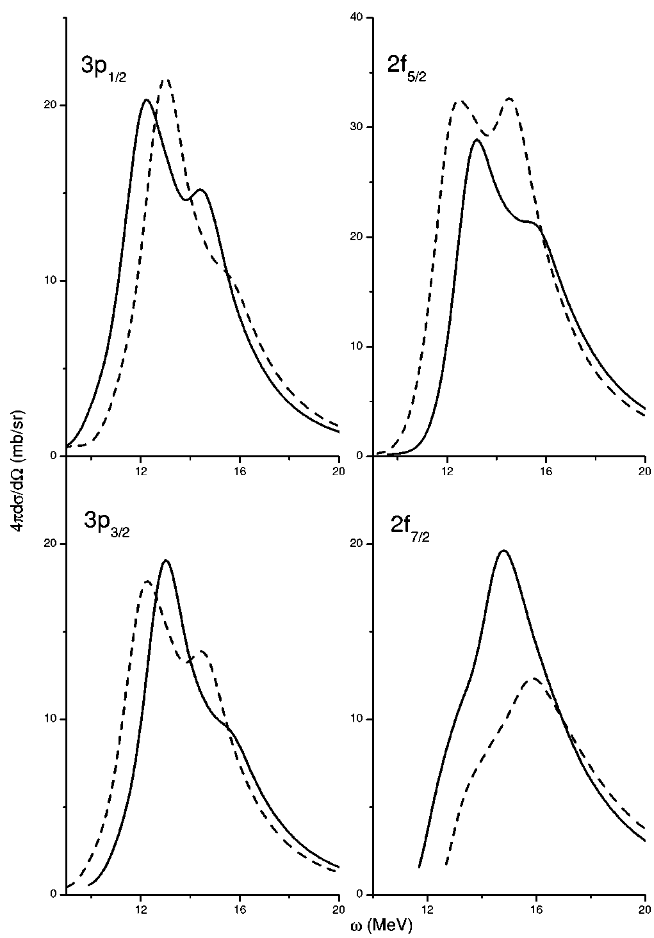

FIG. 5. The calculated partial cross sections at 90° multiplied by 4π of the (γ,n) reaction with population of some single-hole states in ^{207}Pb as functions of photon energy.

TABLE III. Calculated branching ratios for direct neutron decay of the GDR in ^{208}Pb.

	m^*/m	Final single-hole states					
		$3p_{1/2}$	$2f_{5/2}$	$3p_{3/2}$	$1i_{13/2}$	$2f_{7/2}$	$1h_{9/2}$
b_μ	1.0	2.0	4.4	3.4	1.3	2.5	0.7
(%)	0.9	1.8	3.6	3.1	1.0	1.8	0.4

cross section is multiplied by the experimental spectroscopic factor, S_μ, of the final product-nucleus single-particle state populated after the capture. The factors S_μ are listed in Table II. The calculated cross sections at 90° and the anysotropy parameters $\overline{a}_\mu$ are shown in Figs. 2–4 in comparison with the respective experimental data for the nuclei in question. We also calculate some partial ^{208}Pb(γ,n)-reaction cross sections, $d\overline{\sigma}_\mu/d\Omega$, at 90° with the population of single-hole states in ^{207}Pb (Fig. 5). The direct-nucleon-decay branching ratios, b_μ, for the GDR in ^{208}Pb are calculated according to Eq. (14) using a spectroscopic factor of unity for the final single-hole states in ^{207}Pb. The b_μ values are listed in Table III, and the total branching ratio $b=\Sigma_\mu b_\mu$ is estimated as 14%.

To a certain degree, the branching ratios of Eq. (14) can be considered to be independent of the GDR excitation process. The semimicroscopical approach is also applied to evaluate the total direct-neutron-decay branching ratio, b, for the GDR in ^{48}Ca: this value has been deduced from the ^{48}Ca$(e,e'n)$ reaction cross section [13]. In the analysis, the $E1$ strength function, deduced from the (e,e')-reaction in Ref. [13], is used to determine the parameter κ' (Table I). Unit spectroscopic factors are also used for the final single-hole states $7/2^-$, $1/2^+$, and $3/2^+$ in ^{47}Ca. The calculated value of $b=27\%$ is comparable with the respective experimental value $b^{exp}=39\pm5\%$ [13].

IV. CONCLUDING REMARKS

As compared to the previous attempt of Ref. [12], our results allow us to make several comments on capability of the semimicroscopical approach in describing the simplest photonuclear reactions accompanied by the GDR excitation:

(i) The use of the "$\omega+(i/2)I$ method" to take into account phenomenologically the spreading effect allows us to simplify the calculations of the energy-averaged reaction cross sections and also to account for the nonresonant background. This method can be only used to describe highly excited giant resonances within our approach.

(ii) The isoscalar part of separable momentum-dependent forces is also taken into consideration, and results in the difference of the nucleon effective mass from the free value. It is also seen that the use of the a "realistic" effective mass does not improve the description of the data.

(iii) A reasonable description of two sets of the rather old experimental data on the partial (n,γ) reactions for medium-heavy mass nuclei [17,18] is obtained. Possibly the use of a more elaborate version of the approach [by taking $(N-Z)/A$ corrections into account, the use of realistic momentum-dependent forces, etc.] will lead to better description of the photonuclear reaction data.

(iv) Our consideration of predictions for partial ^{208}Pb(γ,n)-reaction cross section has been partially motivated by the advent of new facilities, such as SPring-8 (based on the use of backward Compton scattering), capable of measuring photonuclear reaction cross sections with high accuracy. Such electromagnetic probes are more efficient for studying the nuclear structure. From this point of view the recent experimental data on the $(e,e'n)$ reaction [13] represents a good example.

ACKNOWLEDGMENTS

The authors are grateful to Dr. G.C. Hillhouse for carefully reading the manuscript and many useful remarks for improvement. This work is partially supported by the Russian Fund for Basic Research (RFBR) under Grant No. 02-02-16655. V.A.R. would like to thank the Graduiertenkolleg "Hadronen im Vakuum, in Kernen und Sternen" (GRK683) for supporting his stay in Tübingen and Professor A. Fäßler for his hospitality.

[1] M. Danos, B.S. Ishkhanov, N.P. Yudin, and R.A. Eramzhyan, Usp. Fiz. Nauk **165**, 1345 (1995) [Phys. Usp. **38**, 1297 (1995)].
[2] N. Auerbach and A. Klein, Nucl. Phys. **A395**, 77 (1983).
[3] N. Van Giai and Ch. Stoyanov, Phys. Lett. B **252**, 9 (1990).
[4] S. Kamerdzhiev *et al.*, Nucl. Phys. **A555**, 90 (1993).
[5] S.E. Muraviev and M.H. Urin, Nucl. Phys. **A572**, 267 (1994).
[6] G.E. Brown, Nucl. Phys. **57**, 339 (1964).
[7] A. Likar and T. Vidmar, Nucl. Phys. **A637**, 365 (1998).
[8] G.A. Chekomazov and M.H. Urin, Phys. Lett. B **354**, 7 (1995).
[9] E.A. Moukhai, V.A. Rodin, and M.H. Urin, Phys. Lett. B **447**, 8 (1999); V.A. Rodin and M.H. Urin, Nucl. Phys. **A687**, 276c (2001); M.L. Gorelik and M.H. Urin, Phys. Rev. C **63**, 064312 (2001).
[10] M.L. Gorelik, S. Shlomo, and M.H. Urin, Phys. Rev. C **62**, 044301 (2000); M.L. Gorelik and M.H. Urin, *ibid.* **64**, 047301 (2001).
[11] B.L. Berman and S.C. Fultz, Rev. Mod. Phys. **47**, 713 (1975); I.N. Boboshin, A.V. Varlamov, V.V. Varlamov, D.S. Rudenko, and M.E. Stepanov, The Centre for Photonuclear Experiment Data, CDFE nuclear data bases, http://depni.npi.msu.su/cdfe, INP preprint 99-26/584, Moscow, 1999.
[12] V.A. Rodin and M.H. Urin, Phys. Lett. B **480**, 45 (2000).
[13] S. Strauch, P. von Neumann-Cosel, C. Rangacharyulu, A.

Richter, G. Schrieder, K. Schweda, and J. Wambach, Phys. Rev. Lett. **85**, 2913 (2000).

[14] A.B. Migdal, *Theory of Finite Fermi Systems and Properties of Atomic Nuclei* (Nauka, Moscow, 1983) (in Russian).

[15] L.D. Landau and E.M. Lifschitz, *Quantum Mechanics* (Pergamon, Oxford, 1976).

[16] C. Mahaux and R. Sartor, Nucl. Phys. **A503**, 525 (1989;)

[17] I. Bergqvist, D.M. Drake, and D.K. McDaniels, Nucl. Phys. **A191**, 641 (1972).

[18] I. Bergqvist, B. Palson, L. Nilsson, A. Lindholm, D.M. Drake, E. Arthur, D.K. McDaniels and P. Varghese, Nucl. Phys. **A295**, 256 (1978).